MCA: Modality Composition Awareness for Robust Composed Multimodal Retrieval

Qiyu Wu*, **Shuyang Cui**, **Satoshi Hayakawa**†, **Wei-Yao Wang**, **Hiromi Wakaki**, **Yuki Mitsufuji**
Sony Group Corporation
{firstname.lastname}@sony.com

arXiv:2510.15543v2 [cs.CL] 5 Oct 2026

Abstract

Multimodal retrieval, which seeks to retrieve relevant content across modalities such as text or image, supports applications from AI search to contents production. Despite the success of separate-encoder approaches like CLIP aligning modality-specific embeddings with contrastive learning, recent multimodal large language models (MLLMs) enable a unified encoder that directly processes composed inputs. While flexible and advanced, we identify that unified encoders trained with conventional contrastive learning are prone to learn modality shortcut, leading to poor robustness under distribution shifts. We propose a modality composition awareness framework to mitigate this issue. Concretely, it consists of a preference loss enforces multimodal embeddings to outperform their unimodal counterparts, and a composition regularization objective aligns multimodal embeddings with prototypes composed from its unimodal parts. These objectives explicitly model structural relationships between the composed representation and its unimodal counterparts. Experiments on various benchmarks show gains in out-of-distribution retrieval, highlighting modality composition awareness as a effective principle for robust composed multimodal retrieval when utilizing MLLMs as the unified encoder.

1 Introduction

Multimodal retrieval, which aims to retrieve semantically relevant contents across multiple modalities such as text, image and audio, is a fundamental task in various information fields. Its applications span a wide range of domains, such as text-vision retrieval (Huynh et al., 2025; Wang et al., 2021), music retrieval (Doh et al., 2023), product search (Goenka et al., 2022; Zhu et al., 2024b), and multimodal retrieval-augmented generation (Yasunaga et al., 2023; Ghosh et al., 2024; Yang et al., 2024; Jeong et al., 2025). The core ability of multimodal retrieval is to represent multimodal inputs in a shared and comparable embedding space. A prevailing approach to this problem is to adopt unimodal encoders and align the encoded embeddings through contrastive learning (CL). Models following this separate-encoder paradigm, such as CLIP (Radford et al., 2021) and CLAP (Elizalde et al., 2023), have demonstrated the effectiveness of CL, achieving strong performance across various multimodal retrieval tasks. On the other hand, with the rapid development of multimodal large language models (MLLMs) (Alayrac et al., 2022; Li et al., 2023; Bai et al., 2023; Chu et al., 2023; Liu et al., 2023a; Chen et al., 2024), there has been growing interest in employing MLLMs as encoders for multimodal retrieval (Jiang et al., 2024; Zhang et al., 2024b; Huang et al., 2025; Jiang et al., 2025). Unlike separate-encoder frameworks, MLLMs are capable of processing inputs from different modalities, as well as their compositions, within a unified architecture, providing several advantages such as a shared semantic space across modalities, flexible handling of composed queries and documents, e.g., text+image, and the ability to leverage powerful pretrained representations including rich language knowledge and multimodal understanding.

However, this flexibility also makes the model more prone to **modality shortcut learning**. Since all modalities are jointly processed within a shared encoder, the training loss can be minimized by over-relying on the stronger modality signal, while ignoring the complementary one. An example in Figure 1 illustrates that the model suffers from modality shortcuts when processing highly similar images, while ignoring the textual instruction: "put up convertible roof, remove snow, place SUV standing on flat asphalt". Hence, the architecture shift from separate-encoder to unified-encoder makes

*Corresponding to: qiyu.wu@sony.com.
†Currently at The University of Tokyo. Work done while at Sony Group Corporation.

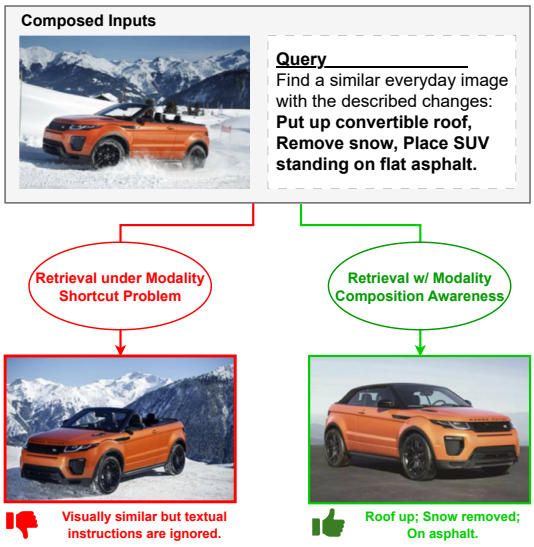

Figure 1: Illustration of modality shortcut problem in multimodal retrieval. Given the inputs consists of an image and textual instruction, **left**: baseline model trained with conventional CL loss retrieve a visually similar image, focusing too much on vision modality; **right**: model trained with modality composition awareness retrieves the relevant image following the instruction.

the direct application of conventional CL objective to unified MLLM encoders limiting to robustness. Furthermore, the modality shortcut issue naturally extends to scenarios involving multiple modalities, particularly as recent work aims to unify various modalities into a single framework (Girdhar et al., 2023; Zhu et al., 2024a; Xu et al., 2025). As the number of modalities increases, so does the risk of the model collapsing to rely on a single dominant modality, making explicit modality composition-aware constraints crucial for robust generalization.

We argue that **modality composition** is the key to mitigate this issue. In this paper, we propose a *modality composition awareness* (MCA) framework that modeling the structural relationship between multimodal and unimodal representations, as shown in Figure 2. MCA consists of two complementary objectives from the preference and consistency perspective, respectively. First, a *preference loss* enforces that the embeddings of a multimodal composition should be more discriminative than any of its unimodal counterparts, thereby discouraging modality shortcut learning. Second, a *composition regularization* objective encourages the consistency between the composed embedding produced by the unified encoder and a compositional prototype constructed from its unimodel embeddings, ensuring that composed representations remain grounded in their constituent modalities. Together, these objectives explicitly model the structural relationship between multimodal and unimodal inputs, leading to more robust representation. Figure 7b visualizes the representation learned with MCA. It demonstrates that composed queries, unimodal queries and targets have a clearer boundary, showing that MCA reduces shortcut reliance.

To comprehensive evaluate MCA, we conduct extensive experiments on both in-domain (IND) and OOD benchmarks, covering retrieval and grounding tasks. The results demonstrate the MCA improves robustness with OOD improvements under distribution shifts while maintaining IND performance. Through ablations, we show that both the preference and regularization components contribute complementary benefits. In addition, we also highlight the interaction between input richness and the strength of our proposed losses. Those results suggest that explicitly modeling modality composition could be a general principle with broader implications for the unified multimodal retrieval using MLLMs.

2 Related Work

Multimodal Retrieval Classical multimodal retrieval typically adopts separate-encoder architectures, learning a text encoder and an image/audio/video encoder whose outputs are aligned in a share space via CL loss. This line of work has achieved strong performance at scale and efficient retrieval (Radford et al., 2021; Li et al., 2022; Zhai et al., 2023). Beyond unimodal inputs, composed retrieval focuses inputs with multiple modalities, such as text+image or text+audio, which better capture user intent in real-world scenarios. This setting has been studied in contexts like text-guided image retrieval (Yu et al., 2016), fashion production search (Wu et al., 2021) and multimodal modification tasks (Liu et al., 2021b). Separate-encoder approaches are principally designed for unimodal queries. When the query or candidate is a composition of modalities, an extra fusion module (Wei et al., 2024; Huynh et al., 2025) has to be trained to fuse the modalities. While these methods demonstrate the feasibility of handling composed queries, they are typically build upon conventional CL loss and do not model the cross-modal interaction between the modalities, leading to a performance sacrifice (Huang et al., 2025). Specif-

ically, UniIR (Wei et al., 2024) fuses unimodal embeddings to enable dual-encoders for composed retrieval, while CoLLM (Huynh et al., 2025) synthesizes composed inputs to augment training data. In contrast, MCA constructs compositional prototypes from unimodal parts within each sample as regularization, specifically targeting the modality shortcut problem in unified MLLM encoders, and this issue is not discussed by prior works.

MLLMs for Retrieval Recent MLLMs extend pretrained LLMs with multimodal adapters or cross-modal modules, enabling an integrated architecture to process and understand over text images, audios and videos (Alayrac et al., 2022; Li et al., 2023; Bai et al., 2023; Chu et al., 2023; Liu et al., 2023a; Chen et al., 2024). Given the unified processing of multiple modalities and rich pre-learned knowledge, MLLMs are increasingly applied to retrieval tasks, especially composed retrieval. Most approaches adapt the unified encoder directly with contrastive learning for embedding-based retrieval (Jiang et al., 2024; Zhang et al., 2024b; Huang et al., 2025; Jiang et al., 2025), while others employ MLLMs as re-rankers for the later re-ranking (Lin et al., 2024). In this work, we study the embedding-based approaches. An advantage of MLLMs for retrieval is the capability of jointly understanding contents in multiple modalities with a unified encoder. However, adopting the unified encoder in contrastive learning could also lead to shortcut learning (Geirhos et al., 2020; Wu et al., 2022). As a result, these recent methods generally inherit conventional contrastive loss and therefore remain vulnerable to modality shortcut when handling composed inputs. Orthogonal to these previous works, we firstly study the modality shortcut problem in this setting and our proposed MCA framework mitigates issue by introducing modality composition-aware objectives that can be easily integrated with MLLM-based retriever to enhance the robustness.

3 Methodology

3.1 Preliminary: MLLM Embedding

Multimodal retrieval aims to search for target documents by a given query. The embedding model, which is central to multimodal retrieval and the focus of our approach, is introduced in this section with the encoding process and training objectives.

Unified Multimodal Encoder Unlike conventional separate-encoder methods such as CLIP (Radford et al., 2021; Zhai et al., 2023), we study the approaches (Lin et al., 2024; Jiang et al., 2024; Zhang et al., 2024b; Huang et al., 2025; Jiang et al., 2025) using a *unified encoder* $f_\theta(\cdot)$, such as a MLLM. Formally, given an input x that could comprises multiple modalities, $f_\theta(\cdot)$ encodes the input into a shared space as: $\mathbf{h} = f_\theta(x)$, where $\mathbf{h} \in \mathbb{R}^d$ is the embedding in d dimensions. In addition, $f_\theta(\cdot)$ includes the necessary processes such as tokenization and pooling, and we omit those details because it does not affect the modeling.

Contrastive Learning Then we can obtain the embedding of a query or document by the unified encoder. Prior works usually adopt the conventional CL loss to align the representations of queries and documents. To achieve this, we first define a function $\text{sim}_\theta(\cdot,\cdot)$ to measure the similarity between two inputs x and y as follows,

$$\text{sim}_\theta(x, y) := \frac{\text{sim}[f_\theta(x), f_\theta(y)]}{\tau}, \quad (1)$$

where τ is the contrastive temperature parameter. As $f_\theta(\cdot)$ is a unified encoder, x and y can be any modalities or the composition of them. Next, the CL objective (Radford et al., 2021) is optimized for aligning the query and positive document. Given the dataset $\mathcal{D}$ that is constructed by queries and documents, in which each query is paired with its positive document, the CL loss can be formalized as follows,

$$\mathcal{L}^{\text{CL}} = \mathbb{E}_{x,y^+,Y\sim\mathcal{D}}\left[-\log \frac{e^{\text{sim}_\theta(x,y^+)}}{e^{\text{sim}_\theta(x,y^+)}+\sum_{y\in Y} e^{\text{sim}_\theta(x,y)}}\right] \quad (2)$$

where x is the query, y^+ is the paired positive document and Y is the batch of negative documents. By doing so, all examples are encoded into a shared space, within which the query is expected to be pulled closer to the positive document but pushed away from negative ones.

3.2 MCA: Multimodal Embedding with Modality Composition Awareness

Although the conventional CL has demonstrated remarkable effectiveness in retrieval (Radford et al., 2021; Baldrati et al., 2022; Liu et al., 2023c), it is inherently designed under the separate-encoder paradigm, where each modality is encoded independently and alignment is enforced at the representation level. With the rapid development of

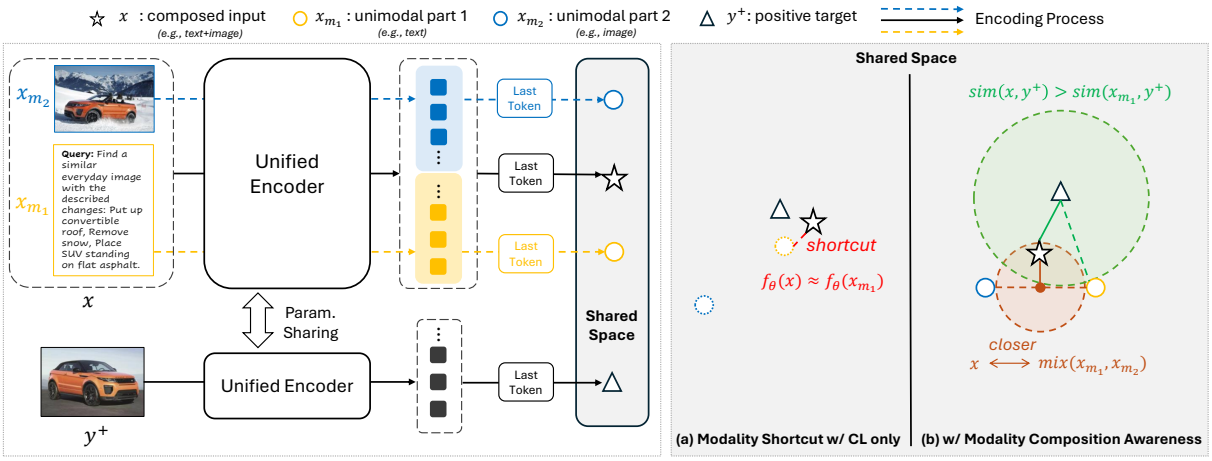

Figure 2: Modality Composition Awareness (MCA, §3.2). Unimodal parts are shown as dotted circles when not explicitly produced. **(a)** Training with vanilla CL: the composed embedding can be close to the target but still align disproportionately with one unimodal part, leading to modality shortcuts. **(b)** Training with CL and MCA: the composed embedding is explicitly constrained to be closer to the target than any of its unimodal parts by MCP (§3.2.1), and anchored to a compositional prototype mixed (Equation 5) from unimodal embeddings by MCR (§3.2.2) to mitigate modality shortcut.

MLLMs, the utilization of unified encoder for retrieval is becoming promising (Jiang et al., 2024; Zhang et al., 2024b; Huang et al., 2025; Jiang et al., 2025). However, those MLLM-based approaches still use conventional CL as the training objective, which is less adequate under composed scenario, where queries or documents may consist of multiple modalities. Such approaches enable models to naturally handle composed inputs within a unified architecture, which could lead to modality shortcut learning as we introduced in §1. Hence, a robust multimodal retrieval paradigm, particularly one that leverages MLLMs and adapts to a wider range of composed scenarios, requires not only aligning across modalities, but also explicitly modeling the *modality composition*.

Consequently, we propose *Modality Composition Awareness* to mitigate this issue. It consists of two components: (1) *Modality Composition Preference* (MCP, §3.2.1) and (2) *Modality Composition Regularization* (MCR, §3.2.2). These two training objectives are illustrated in Figure 2 and will be introduced in the following sections. We first formalize the notation of modalities as $\mathcal{M}$[1]. Given a composed input x, we define the set of its unimodal counterparts as follows,

$$\mathcal{U}(x) := \{x_m \mid m \in \mathcal{M}_x\}, \tag{3}$$

where $\mathcal{M}_x \subset \mathcal{M}$ is the modality set of x, and x_m denotes its unimodal part for modality m. For example, if x comprises text and image modalities, then $\mathcal{U}(x) = \{x_{\text{text}}, x_{\text{image}}\}$.

The modality shortcut problem can be formalized as $f_\theta(x) \approx f_\theta(x_m)$ *regardless of other modalities* after the optimization. In such a case the model only learns unimodal representation even composed inputs are provided. Formally, this key characteristic of modality shortcut is that the representation satisfies $f_\theta((x_m, x_{\text{other}})) \approx f_\theta((x_m, x'_{\text{other}}))$, meaning the model ignores variations in the other modality. As a result, when critical information resides in other modality under OOD conditions, the generalization performance could degrade. Note that modality shortcuts only arise when at least one side of the input pair is a composed input. If both the query and document are unimodal, the task reduces to standard cross-modal retrieval with minimal shortcut risk. Therefore, the following proposed losses are only applied when either the query or document is composed.

3.2.1 Modality Composition Preference

We propose a preference loss that explicitly enforces composed inputs to be more discriminative than their unimodal counterparts. Concretely, given a pair where either side is a composed input, we compute similarities between the composed embedding and candidate targets, as well as between its corresponding unimodal parts and the same target.

[1]In this paper, we use text and image as available modalities, i.e., $\mathcal{M} = \{\text{text}, \text{image}\}$, but the definition can be extended to more modalities.

The MCP loss is formalized as,

$$\mathcal{L}^{\text{MCP}} = \mathbb{E}_{x,y^+\sim\mathcal{D}}\left[-\sum_{x_m\in\mathcal{U}(x)}\log\frac{e^{\text{sim}_\theta(x,y^+)}}{e^{\text{sim}_\theta(x_m,y^+)}}\right], \quad (4)$$

where x and y^+ are the paired query-document sampled from dataset $\mathcal{D}$. The MCP loss encourages the composed similarity higher than the unimodal similarities, ensuring that the model leverages complementary signals from multiple modalities rather than relying on one dominant modality. In other words, the loss formulates a preference-style constraint that whenever a composed input and its unimodal counterparts compete on the same retrieval task, the composed representation should be preferred. For symmetry, we compute the loss in two directions, i.e., x is the document and y^+ is the paired query, ensuring the preference is enforced for both query and document representation.

3.2.2 Modality Composition Regularization

In addition to the preference constraint, we further propose MCR loss to encourage the consistency between the composed embedding and a simple prototype composition of its unimodal embeddings. The intuition is that the representation produced by the encoder for a multimodal input should not deviate arbitrarily from the semantic space spanned by its unimodal parts. To this end, we redefine the similarity function as follows,

$$\text{sim}^{\text{mix}}_{\theta,\phi}(x,\mathcal{U}(x')) := \frac{\text{sim}[f_\theta(x),\text{mix}_\phi(\{f_\theta(x'_m)|x'_m\in\mathcal{U}(x')\})]}{\tau}, \quad (5)$$

where x and x' are two inputs to compare. x is the one we want to regularize, and $\mathcal{U}(x')$ denotes the set of unimodal components that we defined in Equation 3. $\text{mix}(\cdot)$ is a mixer module we defined that aggregates multiple unimodal embeddings into a composed prototype $\mathbf{h}' \in \mathbb{R}^d$ with the same output dimension as $f_\theta(\cdot)$. Thus, the redefined similarity function measures the similarities between the composed prototype derived from x' and the composed embedding of x. In addition, to ensure that the regularization does not dominate learning, the mixer is deliberately kept simple, such as mean pooling or gated fusion, so that the encoder must learn to align composed inputs with the composed prototype rather than overfitting to the mixer. For example, we can instantiate the mixer as a modality-wise gated aggregation:

$$\begin{aligned}[\mathbf{g}_1;\ldots;\mathbf{g}_M] &= \text{softmax}_m\left(\mathbf{W}[\mathbf{h}_1;\ldots;\mathbf{h}_M]+\mathbf{b}\right),\\ \text{mix}^{\text{gated}}_\phi(\{\mathbf{h}_m\}_{m=1}^M) &= \sum_{m=1}^{M}\mathbf{g}_m\odot\mathbf{h}_m.\end{aligned} \quad (6)$$

where $\mathbf{h}_m$ is the unimodal embedding of modality m, $\odot$ denotes element-wise multiplication, and softmax_m normalizes the gates across modalities for each embedding dimension.

The MCR loss is then defined as a contrastive objective, where the composed embedding is pulled closer to its mixed prototype than to other in-batch negatives,

$$\mathcal{L}^{\text{MCR}} = \mathbb{E}_{x,X\sim\mathcal{D}}\left[-\log\frac{e^{\text{sim}^{\text{mix}}_{\theta,\phi}(x,\mathcal{U}(x))}}{e^{\text{sim}^{\text{mix}}_{\theta,\phi}(x,\mathcal{U}(x))}+\sum_{x'\in X}e^{\text{sim}^{\text{mix}}_{\theta,\phi}(x,\mathcal{U}(x'))}}\right], \quad (7)$$

where x is a sampled query or document, and X is a batch of composed inputs that could be either queries or documents for symmetry. Intuitively, the MCR loss enforces that the composed embedding remains anchored to the space formed by its constituent unimodal embeddings, thereby reducing the risk of spurious modality shortcut learning. Finally, we combine the CL loss with the two proposed losses. The overall training objective for optimizing θ and ϕ[2] is formulated as,

$$\mathcal{L} = \mathcal{L}^{\text{CL}} + \alpha\times\mathcal{L}^{\text{MCP}} + \beta\times\mathcal{L}^{\text{MCR}}, \quad (8)$$

where α and β are weighting coefficients controlling the relative strength of auxiliary terms. The impact of weighting is discussed in §4.2.

4 Experiments

To evaluate the proposed MCA, we conduct extensive experiments on multimodal retrieval. Since MCA targets modality shortcut in composed retrieval, we focus on retrieval and grounding benchmarks where the target requires joint visual-textual constraints, and the details of datasets and benchmarks are introduced in §A.1. The training settings are introduced in §A.2. For evaluation we consider both IND benchmarks, which share the same distribution as the training data, and OOD benchmarks that test the generalization to unseen compositions, domains and tasks. OOD performance directly evaluates the shortcut learning problem (Geirhos et al., 2020), because the ideal solution generalizes to OOD test sets, but a shortcut-driven model may only performs well on training and IND test sets, which is illustrated in Figure 6. The OOD benchmarks cover two types of tasks: 1) *OOD retrieval* that measures performance under distribution shifts such as domain and modality composition changes,

[2] ϕ is optimized only when the mixer contains learnable parameters.

Method	In-domain Retrieval									OOD Retrieval				Zero-shot Grounding				
	VisDial	CIRR	VisualNews_t2i	VisualNews_i2t	MSCOCO_t2i	MSCOCO_i2t	NIGHTS	WebQA	**Avg.**	OVEN	FashionIQ	EDIS	**Avg.**	MSCOCO	Visual7W-P	RefCOCO	RefCOCO-M	**Avg.**
Dual-Encoder Baselines																		
CLIP (Radford et al., 2021)	30.7	12.6	78.9	79.6	59.5	57.7	60.4	67.5	55.8	41.1	11.4	81.0	44.5	33.8	55.1	56.9	61.3	51.7
OpenCLIP (Cherti et al., 2023)	25.4	15.4	74.0	78.0	63.6	62.1	66.1	62.1	55.8	45.0	13.8	77.5	45.4	34.5	56.3	54.2	68.3	53.3
SigLIP (Zhai et al., 2023)	21.5	15.1	51.0	52.4	58.3	55.0	62.9	58.1	46.7	56.0	20.1	23.6	33.2	46.4	70.1	70.8	50.8	59.5
BLIP2 (Li et al., 2023)	18.0	9.8	48.1	13.5	53.7	20.3	56.5	55.4	39.5	39.3	9.3	54.4	34.4	28.9	52.0	47.4	59.5	46.9
MagicLens (Zhang et al., 2024a)	24.8	39.1	50.7	21.1	54.1	40.0	58.1	43.0	41.3	11.2	1.6	62.6	25.1	22.1	23.4	22.8	35.6	25.9
Unified MLLM Encoder Baselines																		
E5-V (Jiang et al., 2024)	9.2	6.1	13.5	8.1	20.7	14.0	4.2	17.7	11.6	5.9	2.8	26.8	11.8	10.8	14.3	11.9	38.9	18.9
VLM2Vec (Jiang et al., 2025)	80.9	49.9	75.4	80.0	75.7	73.1	65.5	87.6	73.5	56.5	16.2	87.8	53.5	-	-	-	-	-
Fully-controlled Comparison																		
†Qwen2-VL-2B (Wang et al., 2024)	81.3	51.6	75.7	78.6	73.9	71.9	65.6	86.8	73.2	63.0	15.6	84.0	54.2	41.0	60.7	60.3	69.6	57.9
MCA (Ours, 2B)	80.3	50.5	76.3	78.7	74.6	72.1	66.1	86.8	73.2 (Δ 0.0)	66.7	19.3	86.1	**57.4** ($\Delta + 3.2$)	42.7	65.4	65.0	70.9	**61.0** ($\Delta + 3.1$)

Table 1: Overall results. † indicates the baselines reproduced with identical settings, backbone LLMs, and training data, and Δ indicates the difference compared to the completely comparable baselines.

and 2) *OOD grounding* measures cross-task generalization. Both types of tasks require robust modality composition. Detailed evaluation settings are introduced in §A.3.

4.1 Main Results

Overall Results. Our results in Table 1 demonstrate the superior robustness of MCA in OOD retrieval and zero-shot grounding scenarios. Note that some baselines inevitably differ in training data and backbone models. For instance, VLM2Vec was explicitly trained on grounding tasks so it is not zero-shot performance. To isolate the effect of modality composition awareness from other confounding factors, we set up completely fair comparison between MCA and our reproduced Qwen2-VL, which share identical experimental settings. In general, MLLM-based methods outperform dual-encoder models because their unified encoder enables deeper cross-modal understanding, leading to better performance on all scenarios. However, MLLMs can suffer from modality shortcut issues, where the model relies too heavily on one modality as we introduced in §1. Our MCA is designed to address this limitation and further enhance robustness. Specifically, MCA consistently achieves the highest average in OOD retrieval at 57.4, which is 3.2 points higher than the best baseline, showing a strong ability to generalize to unseen domains. In zero-shot grounding, MCA also leads with an average score of 61.0, outperforming the best baseline by 3.1 points, highlighting its advanced compositional understanding and effective transfer to tasks without explicit training. These results illustrate that modality composition awareness not only boosts robustness to distribution shifts but also enables the model to excel in zero-shot scenarios. Importantly, MCA maintains competitive in-domain retrieval performance, matching the best baseline at 73.2. This balance confirms that the gains in robustness do not come at the expense of accuracy on familiar data. More in-domain trade-off analysis is introduced in §A.10.

Loss Breakdown. As MCA consists of two optimization targets, we further analyze the contribution of the two auxiliary losses separately. As shown in Figure 3, both MCP and MCR individually lead to consistent positive gains on OOD benchmarks. Notably, their standalone improvements are relatively smaller. When combined, the two losses yield substantially larger gains of +5.9% on OOD retrieval and 5.4% on zero-shot grounding, over the model trained with only contrastive learning, demonstrating the necessity of applying them together. This observation aligns with our design intuition in §3.2 that MCP encourages preference against unimodal shortcuts while MCR enforces structural consistency, and only their joint application forms the ideal constraint for robust modality composition, as illustrated in Figure 2. On IND benchmarks, all model variants converge to almost identical accuracy levels. Note that the proposed MCA introduces auxiliary losses to enhance model robustness. Therefore, similar in-domain performance compared to the baseline is expected and indicates that the conventional CL is sufficient to make the model well-converged on IND data. The main focus should be on improvements in OOD and zero-shot scenarios. The full numbers of Fig-

ure3 are listed in §A.5.

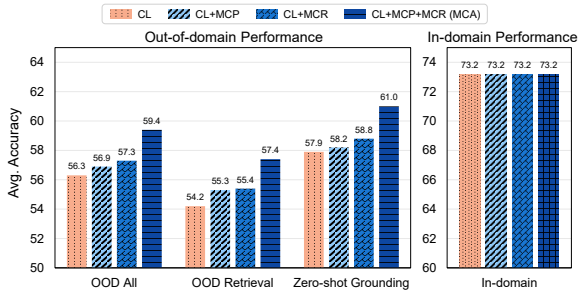

Figure 3: Breakdown of MCA though loss ablation.

4.1.1 Convergence Analysis

To assess the impact of the proposed MCA loss on training dynamics, we perform a convergence analysis by comparing the loss curves and validation performance of both the baseline and the proposed method. This ensures that the improvements on OOD and zero-shot benchmarks are not caused by incomplete optimization or training instability.

Loss Curve We first examine whether the proposed objectives affect the optimization dynamics of the CL loss. Figure 4a compares the CL loss curves with and without MCA during training. Both curves decrease smoothly and monotonically, indicating that introducing MCA does not hinder the convergence of the main contrastive objective. We then analyze the internal loss dynamics of MCA in Figure 4b. The CL, MCP, and MCR losses all converge stably. We note that both MCP and MCR exhibit noticeable fluctuations at the beginning of training, possibly due to the unstable alignment between unimodal and multimodal embeddings in the early stage. Once the representation space becomes more coherent, both losses stabilize at small values. Notably, the MCP loss also serves as a dynamic measure of the modality shortcut gap, since it explicitly encourages the composed query to be more aligned with the target than its unimodal counterparts; therefore, its decrease and stabilization indicate that shortcut behavior is progressively suppressed during training.

Performance Curve To further track model performance during training, we measure the average retrieval accuracy every 100 training steps. Figure 4c shows the IND results, where performance improves steadily and eventually converges to a level comparable to the baseline. In contrast, Figure 4d presents the OOD results, where MCA consistently outperforms the baseline. Moreover, the performance curves reveal that the benefits of MCA appear after a few hundred steps. While IND accuracy converges similarly for models trained with and without MCA, the OOD gap emerges within 500 steps and continues to widen throughout training. This suggests that MCA enhances generalization by mitigating modality shortcuts. Overall, these results show that MCA converges smoothly, with the auxiliary losses acting as regularizers, and leads to consistent improvements on OOD benchmarks where robustness is most critical.

4.2 Input Resolution and MCA Weighting

To better understand the behavior of MCA, we investigate its sensitivity to two critical factors that are relevant: the resolution of image inputs and the weighting of proposed losses. These two factors directly affect the balance between modalities. Specifically, when input information is degraded, the regularization strength might become crucial prevent shortcuts, while richer input information may require lighter regularization to avoid over-constraining the model. Table 2 summarizes the results across three input image resolution and different weighting values. For simplicity, we keep the coefficients of MCP and MCR loss equal, and vary their shared ratio to the CL loss.

MCA Ratio	IND Avg.	OOD Avg.	OOD Retrieval Avg.	Zero-shot Grounding Avg.
Low resolution (128 × 128)				
0	69.7	46.7	42.5	49.9
0.01	69.5 (-0.3%)	44.0 (-5.8%)	37.6 (-11.6%)	48.8 (-2.2%)
0.10	69.3 (-0.6%)	49.5 (+5.9%)	46.8 (+10.1%)	51.4 (+3.0%)
1.00	69.5 (-0.3%)	50.9 (+8.9%)	48.1 (+13.1%)	52.9 (+6.0%)
Mid resolution (672 × 672)				
0	72.0	53.9	49.9	56.8
0.01	71.3 (-1.0%)	54.7 (+1.4%)	53.5 (+7.2%)	55.5 (-2.3%)
0.10	71.5 (-0.7%)	54.9 (+1.8%)	51.3 (+2.8%)	57.6 (+1.4%)
1.00	70.9 (-1.6%)	55.8 (+3.5%)	53.9 (+8.0%)	57.3 (+0.8%)
High resolution (1344 × 1344)				
0	73.2	56.3	54.2	57.9
0.01	73.2 (+0.0%)	59.4 (+5.5%)	57.4 (+5.9%)	61.0 (+5.4%)
0.10	73.0 (-0.3%)	56.6 (+0.5%)	53.4 (-1.5%)	59.1 (+2.0%)
1.00	73.2 (+0.0%)	58.3 (+3.5%)	57.0 (+5.1%)	59.3 (+2.4%)

Table 2: Impact of weighting MCA on varying input image resolution. Darker colors denote larger deviations from the vanilla CL.

Overall, we observe that higher resolution consistently yield stronger performance as expected, since richer visual detail provides more reliable visual grounding. Interestingly, the relative gain from MCA grows larger as the resolution decreases. In lower resolution setting, where visual information

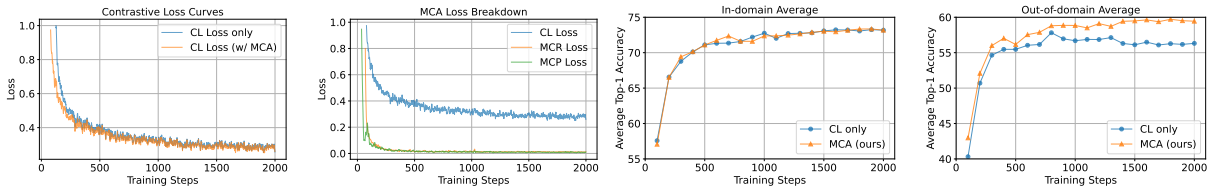

(a) CL loss curve. (b) MCA components loss. (c) IND performance curve. (d) OOD performance curve.

Figure 4: Convergence analysis of MCA. For a fair comparison, the y-axis range for the loss is set to 0–1, and the range for benchmark performance is consistently set to 20.

is degraded and the risk of modality shortcuts is higher, MCA provides significant improvements by enforcing the use of complementary textual cues. This patter suggest that MCA is potentially more effective in scenarios with *imbalanced modality* quality, where it helps the model resist collapsing onto a single modality and instead maintain faithful composition. Nevertheless, we also observe notable exceptions. In particular, under low-resolution inputs with very small weights 0.01, the model performs significantly worse than the vanilla CL baseline on OOD benchmarks. The possible reason is, the additional losses introduce small but inconsistent gradients, which are amplified by the noisy low-resolution image representations. As a result, the model is shifted away from the vanilla CL optimum without receiving sufficient corrective signal, causing a collapse even more severe than the baseline. In the mid-resolution setting, we also observe a modest degradation on IND benchmarks. this can be interpreted as the classic bias-variance trade-off. This degradation remains small, and the overall benefit of MCA becomes more evident when robustness is prioritized.

In addition, the results generally highlight an interaction between input richness and the strength of MCA regularization. When visual inputs are degraded, the risk of modality shortcuts is amplified, and stronger weighting is required for MCA to be effective. In contrast, when inputs provide richer information, the model relies less on shortcuts and lighter weighting suffices to stabilize the training. This trend suggests a practical guideline: the richer the input information, the smaller the weighting can lead to a better generalization, whereas weaker inputs demand stronger regularization to preserve robust modality composition.

4.3 Mixer Implementation

To examine the effect of different implementations of the mixer that defined in Equation 5, we compare several simple modules, including the gated fusion module by default, the non-parametric mean pooling and the multimodal factorized bilinear pooling (MFB) (Yu et al., 2017). All mixer choices introduce only a negligible number of additional parameters, ensuring that the observed gains are not due to increased model capacity. As shown in Table 3, the choice of mixer has little effect on IND benchmarks, suggesting that MCA does not alter the standard retrieval behavior. However, the improvements differ in OOD settings. Both gated fusion and MFB variants yield improvements over the CL-only baseline, demonstrating the explicitly anchoring composed embeddings to the prototype from their unimodal parts is beneficial. In contrast, the mean pooling provides only marginal improvements and even slightly degrades perfromance on cross-task grounding. This indicates that overly simple designs may be insufficient in practice to construct the prototype from unimodal embeddings. Among them, the default gated fusion achieves the best performance. Above experiments suggest that the effectiveness of MCR does not heavily rely on the specific choice of the mixer, but rather on the general principle of enforcing compositional consistency, although the gain could vary depending on the mixer implementation.

Mixer	In-domain Avg.	OOD Avg.	OOD Retrieval Avg.	Zero-shot Grounding Avg.
Vanilla CL	73.2	56.3	54.2	57.9
Mean Pooling	73.3 (+0.1%)	56.5 (+0.3%)	54.8 (+1.1%)	57.8 (-0.2%)
Gated Fusion	73.2 (+0.0%)	59.4 (+5.5%)	57.4 (+5.9%)	61.0 (+5.4%)
MFB	73.0 (-0.2%)	57.7 (+2.4%)	54.6 (+0.7%)	60.0 (+3.6%)

Table 3: Impact of mixer. Darker colors denote larger deviations from the vanilla CL.

4.4 Qualitative analysis

Figure 5 presents qualitative comparisons between the baseline, i.e., training with only contrastive learning, and MCA model, to highlight the behav-

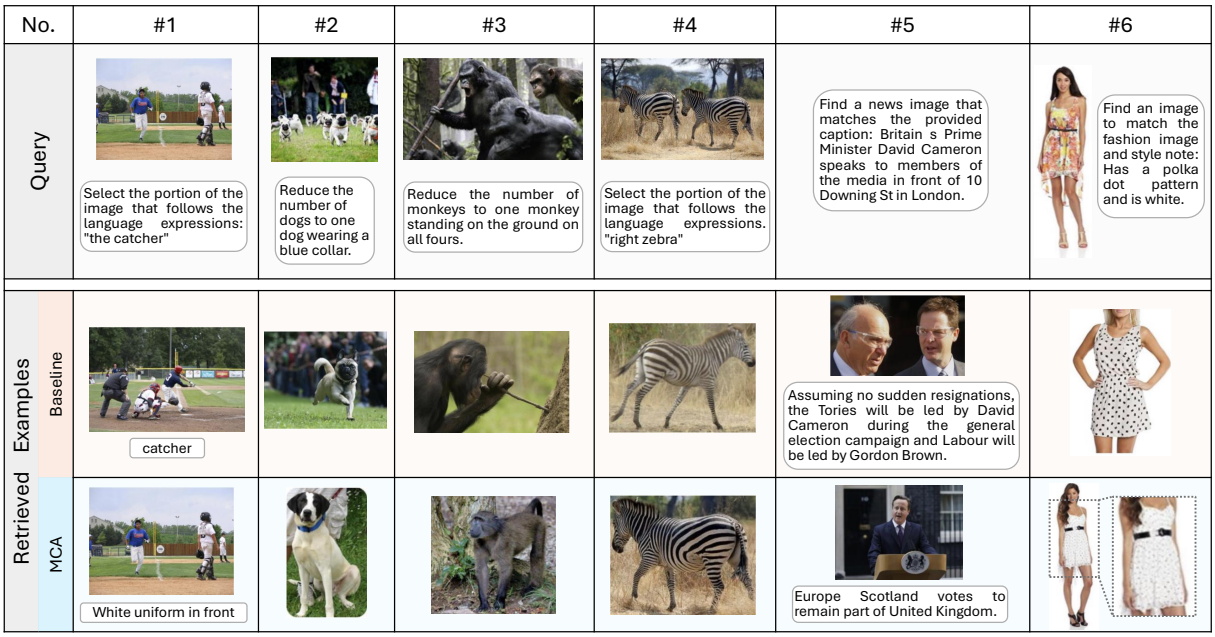

Figure 5: Qualitative examples. The central part of the retrieved image by MCA for #6 is zoomed in for a better visibility.

ior of modality shortcut. Across diverse cases from multiple benchmarks, the baseline fails by relying on partial cues in dominant modalities. For example, in #1 it select an irrelevant baseball scene because of the word *"catcher"*, ignoring the visual grounding on the original image. In contrast, MCA retrieves the image with textual description *"white uniform in front"*. In #2 and #3, the baseline retrieves examples relying on image similarity only, but ignoring the textual instructions. *"wearing a blue collar"* in #2 and *"standing on the ground on all fours"* in #3 are not reflected, while MCA grasps those information. In #4, the baseline mistakenly retrieves a zebra facing right, over-relying on the text cue and failing to ground the original image. MCA, by contrast, localizes the *"right zebra"* in the scene. In the news retrieval case #5, the query mentions *"David Cameron speaking in front of 10 Downing St"*, yet the baseline retrieves the pair containing *"David Cameron"* in both text and image but ignores the *" speaking in front of 10 Downing St"*. MCA composes the texts and image thus finds the best match. Similarly, in the fashion example #6, the baseline retrieves an image satisfying *"polka dot and white"* but ignoring the original clothing style in the image. In contrast, MCA integrates both modalities and selects the desired target. Those examples demonstrate how MCA mitigate modality shortcuts with the potential for more robust multimodal retrieval under various composed scenarios. In addition, we also present visualization of learned embeddings demonstrating that MCA effectively reduce the modality shortcut in §A.8.

5 Conclusion

In this work, we introduced modality composition awareness (MCA) for robust multimodal retrieval. By explicitly modeling the relationship between unimodal and multimodal inputs, MCA incorporates two objectives: (1) modality composition preference, which discourages modality shortcuts by ensuring that composed representations are more discriminative than unimodal ones, and (2) modality composition regularization , which stabilizes embedding by aligning multimodal presentations with compositional prototypes. Extensive empirical experiments across IND and OOD benchmarks demonstrate that MCA achieves consistent gains under distribution shifts and unseen zero-shot tasks, while maintaining comparable IND accuracy. These results highlight MCA as an effective principle for mitigating modality shortcut problem when using MLLMs as unified encoder and improving generalization in multimodal retrieval.

Limitations

While our proposed modality composition awareness show consistent improvements across various OOD benchmarks, several limitations remain. First, the design of our losses assume that modality shortcuts primarily arise when composed inputs are present, and thus the framework is not directly applied to purely unimodal queries. This assumption may overlook shortcut phenomena that could still exist in separate-encoder approaches, although the risk is notably lower. Second, the experimental results still show that our proposed MCA could lead to performance degradation under particular weighting and input resolution setting. Although rare, this phenomenon suggests that it may requires setting adjust to make the proposed loss work in practice. Third, in this work we only explore simple mixer implementation for fair comparison, and extending the design to richer mixers is an interesting open direction. Lastly, although we have identified and studied the modality shortcut problem for vision-text, due to the lack of composed training data and benchmarks, the generalization to broader modalities, e.g., audio, has not yet been validated. In §A.6 we present omni-modal generalization experiment but it is not thorough enough as most settings are empirically set.

Ethical Considerations

This work focuses on improving multimodal representation learning by mitigating modality shortcut problem. Our experiments are conducted entirely on publicly available datasets and model checkpoints. Our method does not directly generate new contents but instead focuses on retrieval, as a result, it poses minimal risk of misuse in generating harmful or deceptive contents. Nevertheless, we emphasize the importance of responsible use of the retrieval model because the MLLMs could have unexpected biases.

References

Jean-Baptiste Alayrac, Jeff Donahue, Pauline Luc, Antoine Miech, Iain Barr, Yana Hasson, Karel Lenc, Arthur Mensch, Katherine Millican, Malcolm Reynolds, and 1 others. 2022. Flamingo: a visual language model for few-shot learning. *Advances in neural information processing systems*, 35:23716–23736.

Jinze Bai, Shuai Bai, Yunfei Chu, Zeyu Cui, Kai Dang, Xiaodong Deng, Yang Fan, Wenbin Ge, Yu Han, Fei Huang, and 1 others. 2023. Qwen technical report. *arXiv preprint arXiv:2309.16609*.

Alberto Baldrati, Marco Bertini, Tiberio Uricchio, and Alberto Del Bimbo. 2022. Effective conditioned and composed image retrieval combining clip-based features. In *Proceedings of the IEEE/CVF conference on computer vision and pattern recognition*, pages 21466–21474.

Yingshan Chang, Mridu Narang, Hisami Suzuki, Guihong Cao, Jianfeng Gao, and Yonatan Bisk. 2022. Webqa: Multihop and multimodal qa. In *Proceedings of the IEEE/CVF conference on computer vision and pattern recognition*, pages 16495–16504.

Zhe Chen, Jiannan Wu, Wenhai Wang, Weijie Su, Guo Chen, Sen Xing, Muyan Zhong, Qinglong Zhang, Xizhou Zhu, Lewei Lu, and 1 others. 2024. Internvl: Scaling up vision foundation models and aligning for generic visual-linguistic tasks. In *Proceedings of the IEEE/CVF conference on computer vision and pattern recognition*, pages 24185–24198.

Mehdi Cherti, Romain Beaumont, Ross Wightman, Mitchell Wortsman, Gabriel Ilharco, Cade Gordon, Christoph Schuhmann, Ludwig Schmidt, and Jenia Jitsev. 2023. Reproducible scaling laws for contrastive language-image learning. In *Proceedings of the IEEE/CVF conference on computer vision and pattern recognition*, pages 2818–2829.

Yunfei Chu, Jin Xu, Xiaohuan Zhou, Qian Yang, Shiliang Zhang, Zhijie Yan, Chang Zhou, and Jingren Zhou. 2023. Qwen-audio: Advancing universal audio understanding via unified large-scale audio-language models. *arXiv preprint arXiv:2311.07919*.

Abhishek Das, Satwik Kottur, Khushi Gupta, Avi Singh, Deshraj Yadav, José MF Moura, Devi Parikh, and Dhruv Batra. 2017. Visual dialog. In *Proceedings of the IEEE conference on computer vision and pattern recognition*, pages 326–335.

SeungHeon Doh, Minz Won, Keunwoo Choi, and Juhan Nam. 2023. Toward universal text-to-music retrieval. In *ICASSP 2023-2023 IEEE International Conference on Acoustics, Speech and Signal Processing (ICASSP)*, pages 1–5. IEEE.

Benjamin Elizalde, Soham Deshmukh, Mahmoud Al Ismail, and Huaming Wang. 2023. Clap learning audio concepts from natural language supervision. In *ICASSP 2023-2023 IEEE International Conference on Acoustics, Speech and Signal Processing (ICASSP)*, pages 1–5. IEEE.

Stephanie Fu, Netanel Tamir, Shobhita Sundaram, Lucy Chai, Richard Zhang, Tali Dekel, and Phillip Isola. 2023. Dreamsim: Learning new dimensions of human visual similarity using synthetic data. In *Advances in Neural Information Processing Systems*, volume 36, pages 50742–50768.

Robert Geirhos, Jörn-Henrik Jacobsen, Claudio Michaelis, Richard Zemel, Wieland Brendel,

Matthias Bethge, and Felix A Wichmann. 2020. Shortcut learning in deep neural networks. *Nature Machine Intelligence*, 2(11):665–673.

Sreyan Ghosh, Sonal Kumar, Chandra Kiran Reddy Evuru, Ramani Duraiswami, and Dinesh Manocha. 2024. Recap: Retrieval-augmented audio captioning. In *ICASSP 2024-2024 IEEE International Conference on Acoustics, Speech and Signal Processing (ICASSP)*, pages 1161–1165. IEEE.

Rohit Girdhar, Alaaeldin El-Nouby, Zhuang Liu, Mannat Singh, Kalyan Vasudev Alwala, Armand Joulin, and Ishan Misra. 2023. Imagebind: One embedding space to bind them all. In *Proceedings of the IEEE/CVF conference on computer vision and pattern recognition*, pages 15180–15190.

Sonam Goenka, Zhaoheng Zheng, Ayush Jaiswal, Rakesh Chada, Yue Wu, Varsha Hedau, and Pradeep Natarajan. 2022. Fashionvlp: Vision language transformer for fashion retrieval with feedback. In *Proceedings of the IEEE/CVF Conference on Computer Vision and Pattern Recognition*, pages 14105–14115.

Edward J Hu, yelong shen, Phillip Wallis, Zeyuan Allen-Zhu, Yuanzhi Li, Shean Wang, Lu Wang, and Weizhu Chen. 2022. LoRA: Low-rank adaptation of large language models. In *International Conference on Learning Representations*.

Hexiang Hu, Yi Luan, Yang Chen, Urvashi Khandelwal, Mandar Joshi, Kenton Lee, Kristina Toutanova, and Ming-Wei Chang. 2023. Open-domain visual entity recognition: Towards recognizing millions of wikipedia entities. In *Proceedings of the IEEE/CVF International Conference on Computer Vision*, pages 12065–12075.

Lang Huang, Qiyu Wu, Zhongtao Miao, and Toshihiko Yamasaki. 2025. Joint fusion and encoding: Advancing multimodal retrieval from the ground up. *arXiv preprint arXiv:2502.20008*.

Chuong Huynh, Jinyu Yang, Ashish Tawari, Mubarak Shah, Son Tran, Raffay Hamid, Trishul Chilimbi, and Abhinav Shrivastava. 2025. Collm: A large language model for composed image retrieval. In *Proceedings of the Computer Vision and Pattern Recognition Conference*, pages 3994–4004.

Soyeong Jeong, Kangsan Kim, Jinheon Baek, and Sung Ju Hwang. 2025. Videorag: Retrieval-augmented generation over video corpus. *arXiv preprint arXiv:2501.05874*.

Ting Jiang, Minghui Song, Zihan Zhang, Haizhen Huang, Weiwei Deng, Feng Sun, Qi Zhang, Deqing Wang, and Fuzhen Zhuang. 2024. E5-v: Universal embeddings with multimodal large language models. *arXiv preprint arXiv:2407.12580*.

Ziyan Jiang, Rui Meng, Xinyi Yang, Semih Yavuz, Yingbo Zhou, and Wenhu Chen. 2025. VLM2vec: Training vision-language models for massive multimodal embedding tasks. In *The Thirteenth International Conference on Learning Representations*.

Sahar Kazemzadeh, Vicente Ordonez, Mark Matten, and Tamara Berg. 2014. Referitgame: Referring to objects in photographs of natural scenes. In *Proceedings of the 2014 conference on empirical methods in natural language processing (EMNLP)*, pages 787–798.

Junnan Li, Dongxu Li, Silvio Savarese, and Steven Hoi. 2023. Blip-2: Bootstrapping language-image pre-training with frozen image encoders and large language models. In *International conference on machine learning*, pages 19730–19742. PMLR.

Junnan Li, Dongxu Li, Caiming Xiong, and Steven Hoi. 2022. Blip: Bootstrapping language-image pre-training for unified vision-language understanding and generation. In *International conference on machine learning*, pages 12888–12900. PMLR.

Sheng-Chieh Lin, Chankyu Lee, Mohammad Shoeybi, Jimmy Lin, Bryan Catanzaro, and Wei Ping. 2024. Mm-embed: Universal multimodal retrieval with multimodal llms. *arXiv preprint arXiv:2411.02571*.

Tsung-Yi Lin, Michael Maire, Serge Belongie, James Hays, Pietro Perona, Deva Ramanan, Piotr Dollár, and C Lawrence Zitnick. 2014. Microsoft coco: Common objects in context. In *European conference on computer vision*, pages 740–755. Springer.

Fuxiao Liu, Yinghan Wang, Tianlu Wang, and Vicente Ordonez. 2021a. Visual news: Benchmark and challenges in news image captioning. In *Proceedings of the 2021 Conference on Empirical Methods in Natural Language Processing*, pages 6761–6771.

Haotian Liu, Chunyuan Li, Qingyang Wu, and Yong Jae Lee. 2023a. Visual instruction tuning. *Advances in neural information processing systems*, 36:34892–34916.

Siqi Liu, Weixi Feng, Tsu-jui Fu, Wenhu Chen, and William Yang Wang. 2023b. Edis: Entity-driven image search over multimodal web content. *arXiv preprint arXiv:2305.13631*.

Zhenghao Liu, Chenyan Xiong, Yuanhuiyi Lv, Zhiyuan Liu, and Ge Yu. 2023c. Universal vision-language dense retrieval: Learning a unified representation space for multi-modal retrieval. In *The Eleventh International Conference on Learning Representations*.

Zheyuan Liu, Cristian Rodriguez-Opazo, Damien Teney, and Stephen Gould. 2021b. Image retrieval on real-life images with pre-trained vision-and-language models. In *Proceedings of the IEEE/CVF international conference on computer vision*, pages 2125–2134.

Alec Radford, Jong Wook Kim, Chris Hallacy, Aditya Ramesh, Gabriel Goh, Sandhini Agarwal, Girish Sastry, Amanda Askell, Pamela Mishkin, Jack Clark, and 1 others. 2021. Learning transferable visual models from natural language supervision. In *International conference on machine learning*, pages 8748–8763. PmLR.

Peng Wang, Shuai Bai, Sinan Tan, Shijie Wang, Zhihao Fan, Jinze Bai, Keqin Chen, Xuejing Liu, Jialin Wang, Wenbin Ge, and 1 others. 2024. Qwen2-vl: Enhancing vision-language model's perception of the world at any resolution. *arXiv preprint arXiv:2409.12191*.

Xiaohan Wang, Linchao Zhu, and Yi Yang. 2021. T2vlad: global-local sequence alignment for text-video retrieval. In *Proceedings of the IEEE/CVF conference on computer vision and pattern recognition*, pages 5079–5088.

Cong Wei, Yang Chen, Haonan Chen, Hexiang Hu, Ge Zhang, Jie Fu, Alan Ritter, and Wenhu Chen. 2024. Uniir: Training and benchmarking universal multimodal information retrievers. In *European Conference on Computer Vision*, pages 387–404. Springer.

Hui Wu, Yupeng Gao, Xiaoxiao Guo, Ziad Al-Halah, Steven Rennie, Kristen Grauman, and Rogerio Feris. 2021. Fashion iq: A new dataset towards retrieving images by natural language feedback. In *Proceedings of the IEEE/CVF Conference on computer vision and pattern recognition*, pages 11307–11317.

Qiyu Wu, Chongyang Tao, Tao Shen, Can Xu, Xiubo Geng, and Daxin Jiang. 2022. PCL: Peer-contrastive learning with diverse augmentations for unsupervised sentence embeddings. In *Proceedings of the 2022 Conference on Empirical Methods in Natural Language Processing*, pages 12052–12066, Abu Dhabi, United Arab Emirates. Association for Computational Linguistics.

Jin Xu, Zhifang Guo, Jinzheng He, Hangrui Hu, Ting He, Shuai Bai, Keqin Chen, Jialin Wang, Yang Fan, Kai Dang, and 1 others. 2025. Qwen2. 5-omni technical report. *arXiv preprint arXiv:2503.20215*.

Mu Yang, Bowen Shi, Matthew Le, Wei-Ning Hsu, and Andros Tjandra. 2024. Audiobox tta-rag: Improving zero-shot and few-shot text-to-audio with retrieval-augmented generation. *arXiv preprint arXiv:2411.05141*.

Michihiro Yasunaga, Armen Aghajanyan, Weijia Shi, Richard James, Jure Leskovec, Percy Liang, Mike Lewis, Luke Zettlemoyer, and Wen-Tau Yih. 2023. Retrieval-augmented multimodal language modeling. In *International Conference on Machine Learning*, pages 39755–39769. PMLR.

Licheng Yu, Patrick Poirson, Shan Yang, Alexander C Berg, and Tamara L Berg. 2016. Modeling context in referring expressions. In *European conference on computer vision*, pages 69–85. Springer.

Zhou Yu, Jun Yu, Jianping Fan, and Dacheng Tao. 2017. Multi-modal factorized bilinear pooling with co-attention learning for visual question answering. In *Proceedings of the IEEE international conference on computer vision*, pages 1821–1830.

Xiaohua Zhai, Basil Mustafa, Alexander Kolesnikov, and Lucas Beyer. 2023. Sigmoid loss for language image pre-training. In *Proceedings of the IEEE/CVF international conference on computer vision*, pages 11975–11986.

Kai Zhang, Yi Luan, Hexiang Hu, Kenton Lee, Siyuan Qiao, Wenhu Chen, Yu Su, and Ming-Wei Chang. 2024a. Magiclens: Self-supervised image retrieval with open-ended instructions. *arXiv preprint arXiv:2403.19651*.

Xin Zhang, Yanzhao Zhang, Wen Xie, Mingxin Li, Ziqi Dai, Dingkun Long, Pengjun Xie, Meishan Zhang, Wenjie Li, and Min Zhang. 2024b. Gme: Improving universal multimodal retrieval by multimodal llms. *arXiv preprint arXiv:2412.16855*.

Bin Zhu, Bin Lin, Munan Ning, Yang Yan, Jiaxi Cui, WANG HongFa, Yatian Pang, Wenhao Jiang, Junwu Zhang, Zongwei Li, Cai Wan Zhang, Zhifeng Li, Wei Liu, and Li Yuan. 2024a. Languagebind: Extending video-language pretraining to n-modality by language-based semantic alignment. In *The Twelfth International Conference on Learning Representations*.

Xinliang Zhu, Sheng-Wei Huang, Han Ding, Jinyu Yang, Kelvin Chen, Tao Zhou, Tal Neiman, Ouye Xie, Son Tran, Benjamin Yao, and 1 others. 2024b. Bringing multimodality to amazon visual search system. In *Proceedings of the 30th ACM SIGKDD Conference on Knowledge Discovery and Data Mining*, pages 6390–6399.

Yuke Zhu, Oliver Groth, Michael Bernstein, and Li Fei-Fei. 2016. Visual7w: Grounded question answering in images. In *Proceedings of the IEEE conference on computer vision and pattern recognition*, pages 4995–5004.

A Appendix

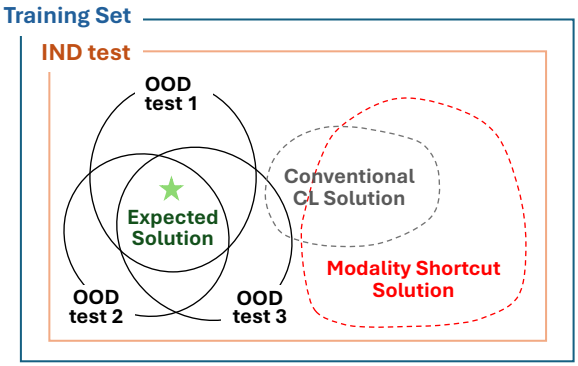

Figure 6: A conceptual diagram showing how OOD benchmarks evaluate modality shortcut.

A.1 Datasets

Training data. We utilize six multimodal retrieval datasets including both *cross-modal* and *composed* tasks for training: MSCOCO (Lin et al., 2014), VisualNews (Liu et al., 2021a), VisDial (Das et al., 2017), CIRR (Liu et al., 2021b), NIGHTS (Fu et al., 2023), and WebQA (Chang et al., 2022). Table 4 shows the number for examples and input modalities of training data. We use the training splits from MMEB[3] without additional curation. All models are trained jointly on the union of these datasets. Although MCA is designed for composed inputs, unimodal training pairs are also included. Each training batch contains a mix of unimodal and composed inputs. This ensures that the model learns basic representation ability for each modality, which is essential modeling of structural relationships among modalities that is required by our objectives.

Benchmarks. We evaluate the models on a range of multimodal retrieval benchmarks, which we group into *IND* and *out-of-domain* (OOD) settings. The IND benchmarks correspond directly to the test splits of the six datasets used for training as mentioned in the previous paragraph and Table 4. Since models that rely on modality shortcuts often exhibit poor generalization, we also assess this issue through robustness under OOD settings. The OOD benchmarks are deliberately selected: OVEN (Hu et al., 2023) combines visual and textual modalities, where each instance consists of an image paired with a visual recognition question, alongside a reference Wikipedia image and its textual description including the title and first 100 tokens that serve as the target candidate for answering the question. FashionIQ (Hu et al., 2023) features a multimodal composition of fashion product images paired with crowd-sourced textual descriptions that specify differences between products, enabling composed image retrieval where a reference image and modification text are combined to retrieve target images. EDIS (Liu et al., 2023b) combines entity-rich text queries with multimodal candidates consisting of news images paired with their headlines, requiring models to understand both textual entities/events and visual content for retrieval. MSCOCO-Grounding (Lin et al., 2014; Jiang et al., 2025) transforms object detection into a multimodal ranking task where queries combine an image with a textual object name to retrieve cropped images of the specified object, with distractors sourced from other objects within the same image and from different images. Visual7W-Pointing (Zhu et al., 2016) combines textual questions with images to establish semantic links between descriptions and image regions, enabling both visual question answering through text-image composition and visual grounding through multimodal object localization. RefCOCO (Kazemzadeh et al., 2014) employs multimodal queries combining images with referring language expressions to identify specific objects, pairing image-text queries to retrieve cropped object images. RefCOCO-Matching (Kazemzadeh et al., 2014; Jiang et al., 2025) uses the same source datasets, while repurposed to match identical image-text compositions where both query and target contain the same object with its referring expression. We directly use the test splits from MMEB[4]. Note that since modality shortcut in MLLMs, the problem we study in this paper, only happens in composed queries or documents, all of our OOD benchmarks focus on *composed retrieval*, in which either query or document side comprise multiple modalities.

A.2 Default training settings

By default, we adopt `Qwen2-VL-2B-Instruct`[5] as the unified encoder backbone. The contrastive temperature τ is set to 0.02. All models are fine-tuned with LoRA (Hu et al., 2022) adapter. Unless other-

[3] https://huggingface.co/datasets/TIGER-Lab/MMEB-train

[4] https://huggingface.co/datasets/TIGER-Lab/MMEB-eval

[5] https://huggingface.co/Qwen/Qwen2-VL-2B-Instruct

Table 4: Statistics of training datasets. I and T are the abbreviation of image and text, respectively.

Dataset	MSCOCO		VisualNews		VisDial	CIRR	NIGHTS	WebQA
Input modalities	I → T	T → I	I → T	T → I	T → I	(I+T) → I	I → I	T → (I+T)
# of training pairs	113K	100K	100K	100K	123K	26K	16K	17K

wise specified, the LoRA rank is set to 8. The overall loss combines conventional contrastive learning and our proposed MCR and MCP terms as introduced in Equation 8, where α and β are weighting hyper-parameters. These auxiliary terms act as regularization signals rather than main training objectives. We empirically adopt a small coefficient between 0.01 and 1.0 to stabilize training. For simplicity, unless the otherwise specified, we tie α and β by setting $\alpha = \beta = 0.01$ by default so that both the preference and regularization losses contribute equally. Following previous work (Jiang et al., 2025), we use AdamW optimizer with a learning rate of $2e-5$ and a linear schedule with warm-up. We also fixed the global batch size as 1024 with gradient accumulation for varying numbers of GPU and memory. The total training steps are 2000 and warm-up steps are 200. The training takes around 200 hours on 8× Nvidia A100 40G. For MCR loss, the mixer function Mix_ϕ in Equation 5 is instantiated as a simple gated fusion module by default, where each unimodal embedding is reweighted by a learnable gating coefficient before aggregation. For ablation, we also experiment with alternatives such as non-parametric mean pooling and multimodal factorized bilinear pooling (Yu et al., 2017) in §4.3. All Qwen2-VL-7B results in §A.7 are reported at the final 2,000-step checkpoint, with MCA weights selected according to the resolution-dependent trend in Section 4.2: $\alpha = \beta = 0.01$ for low resolution and $\alpha = \beta = 1.0$ for mid resolution.

A.3 Default Evaluation Settings

Unless otherwise specified, we report results using the final checkpoint of training for a fair comparison across all methods, as we have verified that the trend is stable across checkpoints in §4.1.1. We report standard retrieval metrics accuracy@1 for all tasks.

A.4 Embedding Visualization

In Figure 7a, we visualize unimodal queries and targets randomly sampled from the CIRR dataset trained with vanilla CL and MCA, respectively. Details of the t-SNE implementation are provided in §A.8. The visualization shows that, under vanilla CL, composed queries (red) are not well separated and frequently cluster close to text-only queries. This suggests that the model tends to exploit modality shortcuts rather than learning robust representations for composed queries. In contrast, with MCA training, composed queries and text-only queries are clearly separated, indicating a more meaningful and robust representation distribution.

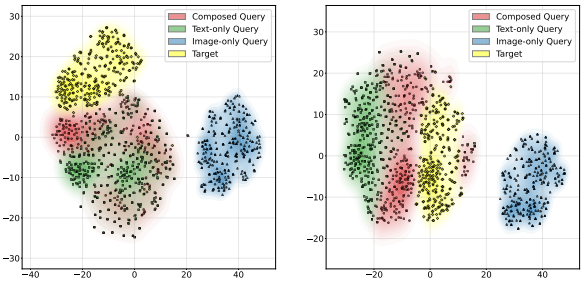

(a) Trained with vanilla CL. (b) Trained with our MCA.

Figure 7: Visualizations of queries and targets.

A.5 Full Loss Ablation Results

Table 5 provides a per-dataset breakdown of the results in Fig.3. All variants maintain nearly identical in-domain retrieval performance, with an average score of 73.2, indicating that the proposed objectives do not sacrifice standard retrieval ability. In contrast, MCP and MCR provide complementary improvements on out-of-domain retrieval and zero-shot grounding. Combining them as MCA yields the strongest overall generalization, improving the OOD retrieval average from 54.2 to 57.4 and the zero-shot grounding average from 57.9 to 61.0. These results suggest that the two components encourage complementary aspects of multimodal composition, leading to more robust transfer beyond the in-domain retrieval setting.

A.6 Generalization Analysis

To better analyze the generalization of MCA on more modalities and different backbone LLM, we conduct an experiment on

Table 5: Per-dataset comparison of different training objectives.

Method	In-domain Retrieval									OOD Retrieval				Zero-shot Grounding				
	VisDial	CIRR	VN-t2i	VN-i2t	COCO-t2i	COCO-i2t	NIGHTS	WebQA	Avg.	OVEN	FashionIQ	EDIS	Avg.	MSCOCO	Visual7W-P	RefCOCO	RefCOCO-M	Avg.
Baseline	81.3	51.6	75.7	78.6	73.9	71.9	65.6	86.8	73.2	63.0	15.6	84.0	54.2	41.0	60.7	60.3	69.6	57.9
CL+MCP	80.6	51.9	74.6	78.4	74.8	73.0	65.6	86.9	73.2	64.1	17.3	84.4	55.3	42.1	64.7	59.0	66.8	58.2
CL+MCR	80.6	49.2	76.5	78.7	75.1	71.6	66.2	88.0	73.2	63.5	18.0	84.6	55.4	41.2	61.1	62.9	69.9	58.8
MCA	80.3	50.5	76.3	78.7	74.6	72.1	66.1	86.8	73.2	**66.7**	**19.3**	**86.1**	**57.4**	**42.7**	**65.4**	**65.0**	**70.9**	**61.0**

	# Tasks	Vanilla CL	MCA	Δ
Overall	67	52.09	**52.91**	+0.82
Composed	28	55.78	**56.96**	+1.18
Non-composed	39	49.45	**50.01**	+0.56
Image composed	18	61.90	**62.81**	+0.91
Video composed	8	43.87	**45.59**	+1.72
Audiovisual composed	2	48.33	**49.80**	+1.47
Image non-composed	18	66.66	**66.74**	+0.08
Video non-composed	15	37.40	**38.81**	+1.41
Audio non-composed	6	**27.92**	27.82	-0.10

Table 6: Omni-modal generalization results on 67 tasks. We report the macro-average Accuracy@1 across tasks. Δ denotes the absolute improvement in percentage points.

Mixer	In-domain Avg.	OOD Avg.	OOD Retrieval Avg.	Zero-shot Grounding Avg.
Low resolution				
Qwen2-VL-7B	62.8	43.6	38.2	47.7
MCA-7B	**71.4** (+8.6)	**55.2** (+11.6)	**49.7** (+11.5)	**59.3** (+11.6)
Mid resolution				
Qwen2-VL-7B	76.1	62.6	60.1	64.5
MCA-7B	**76.4** (+0.3)	**63.6** (+1.0)	**60.3** (+0.2)	**66.1** (+1.6)

Table 7: Category-level average results on Qwen2-VL-7B. OOD Avg. is computed over all seven OOD retrieval and zero-shot grounding tasks. Values in parentheses denote absolute improvements over the corresponding Qwen2-VL-7B baseline.

`Qwen2.5-Omni-3B-Thinker` [6]. This experiment covers 67 tasks grouped according to their input modality and whether either side contains a modality composition. For brevity, we list the complete evaluation datasets without repeating individual citations. **Image composed:** A-OKVQA, CIRR, ChartQA, DocVQA, FashionIQ, GQA, InfographicsVQA, MSCOCO, N24News, OK-VQA, OVEN, RefCOCO, RefCOCO-Matching, ScienceQA, TextVQA, Visual7W, Visual7W-Pointing, and VizWiz. **Image non-composed:** Country211, EDIS, HatefulMemes, ImageNet-1K, ImageNet-A, ImageNet-R, MSCOCO-i2t, MSCOCO-t2i, NIGHTS, ObjectNet, Place365, SUN397, VOC2007, VisDial, VisualNews-i2t, VisualNews-t2i, WebQA, and Wiki-SS-NQ. **Video composed:** ActivityNetQA, Charades-STA, EgoSchema, MVBench, MomentSeeker, NExTQA, QVHighlight, and Video-MME. **Video non-composed:** Breakfast, DiDeMo, DiDeMo-V2T, HMDB51, K700, MSR-VTT, MSR-VTT-V2T, MSVD, MSVD-V2T, SmthSmthV2, UCF101, VATEX, VATEX-V2T, YouCook2, and YouCook2-V2T. **Audio non-composed:** AudioCaps, AudioCaps-A2T, Clotho, Clotho-A2T, MusicCaps, and MusicCaps-A2T. **Audiovisual composed:** VALOR32k-T2VA and VALOR32k-VA2T.

The comparison is fully controlled, following our default training setup, and both models are fine-tuned with LoRA for 1000 steps with a global batch size 768. We set the LoRA rank to 16 and the scaling factor to 32. We use last-token pooling, L2-normalized embeddings, and a contrastive temperature of 0.02. For MCA, we set the weights of both MCP and MCR to 0.001. For MCR, we instantiate Mix_ϕ as non-parametric mean pooling. We report accuracy@1 for each task, and each aggregate result is computed as the unweighted macro-average of task-level accuracy@1 scores. The gains still hold in this experiment, with larger improvements on composed tasks, which is consistent with MCA's design. These results provide additional evidence that MCA can potentially scale to other unified encoder with broader modality coverage.

A.7 Scalability to Model Size.

We further evaluate MCA on Qwen2-VL-7B[7] under both low- and mid-resolution settings, with detailed results reported in Table 7. Under low resolution, the 7B baseline shows clear robustness limitations, while MCA substantially improves all evaluation groups, with gains of +8.6 on in-domain retrieval, +11.5 on OOD retrieval, and +11.6 on zero-shot grounding. Under mid resolution, where the baseline is already much stronger, MCA still provides consistent improvements, especially on zero-shot grounding. This trend is consistent with the observations in § 4.2. When visual inputs are degraded, modality imbalance becomes more severe and the model is more prone to shortcut learning, making composition-aware regularization

[6] https://huggingface.co/Qwen/Qwen2.5-Omni-3B

[7] https://huggingface.co/Qwen/Qwen2-VL-7B

more beneficial. These results show that MCA scales to larger backbones and is particularly effective when visual evidence is constrained.

A.8 tSNE Implementation

In Figure 7a and 7b, we visualize the learned embedding spaces using t-distributed Stochastic Neighbor Embedding (t-SNE) to analyze the distribution characteristics of different query types. Embeddings were extracted from the CIRR dataset, which contains image-text compositions for retrieval tasks. For dimensionality reduction, we employed t-SNE with perplexity=100, 1,000 iterations, and a random seed of 42 to ensure reproducibility. We randomly sampled 300 instances from each embedding type to maintain visual clarity while preserving distribution characteristics. To ensure fair comparison, we used identical sampling indices across all embedding types for baseline and our model. The visualization combines kernel density estimation (KDE) with scatter plots to represent both the overall distribution and individual data points. We implemented a custom transparency gradient for the KDE plots, making low-density regions increasingly transparent to highlight areas of embedding concentration. Different marker shapes distinguish between embedding types: circles for composed queries, squares for text-only queries, triangles for image-only queries, and diamonds for target images. The resulting visualization effectively captures the relationships between different modalities in the embedding space, revealing patterns of overlap and separation between composed, unimodal, and target representations. Comparing Figure 7a and 7b, it clearly indicates that vanilla CL could lead to a over-mixed distribution for composed and text-only embeddings, while MCA learns a more robust representation with a clear boundary among different types of representations with a competitive IND performance and a better OOD performance.

A.9 Training Efficiency

MCA requires additional forward passes during training to compute unimodal embeddings for Equations 4 and 7. Since input sequence length satisfies $\sum_{m\in\mathcal{M}_x} L_m \approx L_{\text{composed}}$, the theoretical FLOPs overhead is approximately two times when text and image are included. Our measured wall-clock time shows 2.26× overhead on 8× A100 GPUs. This overhead can be further reduced because MLLMs are autoregressive, adn the intermediate hidden states for unimodal prefixes are already computed during the composed forward pass and can be reused to obtain unimodal embeddings without separate forward passes. We leave this implementation optimization for future work as it does not affect the model performance. Notably, MCA introduces no additional cost at inference time becasue the mixer is discarded after training.

A.10 In-domain trade-off Analysis

We further analyze the slight per-dataset variations on in-domain benchmarks from a regularization–generalization perspective. Let $\mathcal{H}$ denote the hypothesis space under vanilla CL, and let $\mathcal{H}_{\text{MCA}} \subset \mathcal{H}$ denote the constrained space induced by MCA. For in-domain data where a shortcut solution $h_s \in \mathcal{H}$ achieves low loss, vanilla CL may converge to h_s, while MCA constrains the solution to $h \in \mathcal{H}_{\text{MCA}}$ that better respects modality composition structure. When such shortcuts are incidentally aligned with ground truth, h_s may marginally outperform h on certain in-domain tasks. However, under distribution shift where shortcuts become unreliable, h is expected to generalize better. This reflects an inherent trade-off of regularization-based methods. Specifically, MCA may slightly reduce in-domain flexibility, but it encourages more robust cross-modal composition. Empirically, the in-domain changes remain small, while MCA brings substantially larger gains on OOD retrieval and zero-shot grounding, aligning with its design goal of improving robustness for real-world deployment.

A.11 Diagnostics of Modality Shortcut

In addition to the OOD improvements, to directly verify whether the CL baseline exhibits modality shortcut and whether MCA reduces reliance on a single modality, we add a held-out shortcut diagnostic computed on composed test examples. For each composed input x paired with its positive target y^+, we define the composition margin as

$$\Delta_{\text{comp}}(x, y^+) = \text{sim}[f_\theta(x), f_\theta(y^+)] - \max_{x_m \in \mathcal{U}(x)} \text{sim}[f_\theta(x_m), f_\theta(y^+)], \quad (9)$$

where $\text{sim}[\cdot,\cdot]$ denotes cosine similarity between L2-normalized embeddings. A smaller margin indicates stronger shortcut tendency. We also report MCP loss defined in Equation 4, where a lower value indicates a stronger preference for the composed representation. We compute both diagnostics on a fixed held-out probe containing 200 composed

test examples, with 100 examples from CIRR and 100 examples from NIGHTS. We use the same examples for the step-0 base model, the final vanilla-CL checkpoint, and the final MCA checkpoint.

Model / checkpoint	Composition margin ↑		Held-out MCP loss ↓	
	Value	Δ vs. base	Value	Δ vs. base
Base model, step 0	0.1744	–	0.0667	–
Vanilla CL, final	0.1248	−28.4%	0.0368	−44.8%
MCA, final	**0.2125**	**+21.8%**	**0.0100**	**−85.0%**

Table 8: Held-out modality-shortcut diagnostics on 200 composed test examples from CIRR and NIGHTS. A larger composition margin indicates clearer separation from the strongest unimodal counterpart, while a lower held-out MCP loss indicates a stronger preference for the composed representation.

Table 8 shows that after conventional contrastive training, the composition margin decreases from 0.1744 to 0.1248. This means that although CL improves target matching, the composed query becomes less separated from its strongest unimodal counterpart, indicating stronger shortcut tendency. In contrast, MCA increases the final composition margin to 0.2125. We also observe that the composition-preference violation is much lower for MCA than for CL. Although CL also reduces this violation compared with the base model, MCA reduces it much more substantially, from 0.0368 to 0.0100. This shows that MCA more consistently assigns higher similarity to the composed query than to its unimodal counterparts.

A.12 Failure Case Analysis

We observe a notable failure case in Table 2. Under low-resolution inputs (128×128) with small MCA weight, e.g., 0.01, performance degrades significantly compared to the baseline, specifically, -11.6% on OOD Retrieval. We attribute this to the interaction between modality imbalance and regularization strength. At low resolution, visual representations become unreliable, creating a strong tendency toward text-only shortcuts, which can be a strong attractor in the optimization landscape. Small MCA weight provides insufficient corrective force to escape this attractor. Instead, it can perturb the optimization without guiding the model toward a composition-aware solution. In contrast, higher MCA weights successfully overcome the shortcut attractor by enforcing stronger compositional constraints, yielding improved OOD performance. Based on this analysis, in practice we recommend that when modality quality is imbalanced, for example, degraded images or noisy audio, stronger MCA weights are recommended to counteract shortcut tendencies, and when modalities are balanced and reliable, smaller weights are sufficient.

A.13 Discussion on identity mapping

A potential concern of the proposed composition regularization is that it may admit a degenerate identity-mapping solution, where the composed representation $f_\theta(x_{\text{comp}})$ simply collapses to the mixed unimodal prototype $\text{mix}(f_\theta(x_{\text{text}}), f_\theta(x_{\text{image}}))$. In our formulation, however, the modality composition regularization is not used as a standalone objective, but as a soft regularizer jointly optimized with the retrieval-oriented contrastive and preference losses. Therefore, it only biases the representation toward compositional consistency rather than imposing a hard constraint. Moreover, such a collapse is unlikely in practice due to the strong capacity asymmetry between the MLLM encoder and the lightweight mixer. The encoder, initialized from a pretrained MLLM and updated with parameter-efficient fine-tuning, retains rich cross-modal reasoning capability, whereas the mixer only provides a low-capacity aggregation target. An identity-mapping solution would require the encoder to suppress its cross-modal computation and mimic this simple aggregation rule while still satisfying the retrieval objectives, which is disfavored by the constrained optimization. Thus, the regularization acts as a compositional anchor without dominating the learned representation.

A.14 LLM Usage

During the preparation of this paper, we utilized LLMs to assist with English proofreading. We also use LLM assistant for improving the efficiency of experiments such as organizing job execution scripts. Additionally, we used LLM assistant to support processing experimental results and generating figures.